ЖУРНАЛ СТРУКТУРНОЙ ХИМИИ

2013. Том 54, № 6 *Ноябрь – декабрь* *С. 980 – 985*

UDC 548.737

INSIGHT INTO THE CHEMICAL BONDING AND ELECTROSTATIC POTENTIAL: A CHARGE DENSITY STUDY ON A QUINAZOLINE DERIVATIVE

A. Tojiboev[1], R. Wang[2], F. Pan[2], U. Englert[2], K. Turgunov[3], R. Okmanov[3]

[1]*Department of Physics, Namangan State University, Namangan, Uzbekistan*
E-mail: a_tojiboev@yahoo.com
[2]*Institute of Inorganic Chemistry, RWTH Aachen University, Landoltweg 1, Aachen, Germany*
[3]*S.Yunusov Institute of the Chemistry of Plant Substances, Academy of Sciences Uzbekistan, Tashkent, Uzbekistan*

Received May, 30, 2012 *Revised — March, 12, 2013*

2,3-Trimethylene-3,4-dihydroquinazoline shares the heterocyclic core with natural compounds and synthetic drugs. The hydrochloride of the compound forms excellent dihydrate crystals which have allowed us to collect high-resolution X-ray diffraction data and obtain the experimental charge density. The solid may be understood as built up from pairs of heterocyclic cations and chloride anions; a direct hydrogen bond links the halide to the formally cationic pyrimidine NH group. The hydrate water molecules interact with the anions, forming an infinite chain along the crystallographic *a* axis between the stacks of the heterocyclic cations. Based on the experimental charge density, a dipole moment of 16.1 Debye is calculated for a pair of the hydrogen-bonded quinazolinium cation and the chloride anion in the extended crystal structure.

K e y w o r d s: quinazoline, electronic structure, high-resolution X-ray diffraction, charge density, topological analysis, dipole moment.

INTRODUCTION

Quinazoline represents the heterocyclic core of natural alkaloids and pharmaceutically active ingredients [1—3]. Substituted quinazolines such as doxazosin and prazosin have been commercialized as alpha blockers, and the keto derivative methaqualone is a sedative drug. In addition, quinazolines may act as inhibitors of kinase targets [4] and hence show potential as anti-cancer drugs. For the understanding of their biological activity and potential pharmacological applications, a routine determination of the geometric structure of a compound is not sufficient. The precise knowledge of the electron density is also of paramount importance because the electrostatic potential plays a key role in the process of molecular recognition [5]. In line with these ideas, Luger and coworkers [6] have studied the electron density of a quinazoline-based tyrosine-kinase inhibitor. Recently, the crystal structure of the peganine hydrochloride dihydrate compound has been reported; this alkaloid has been identified as an orally active antileishmanial agent [7]. The closely related target compound of the present study, the alkaloid deoxypeganine (DOP), was isolated from *Peganum harmala* [8]; a chemical diagram of DOP hydrochloride dihydrate **1** is shown in Fig. 1.

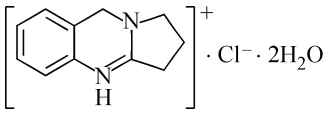

Fig. 1. Chemical diagram of DOP hydrochloride dihydrate ($DOPH^+ Cl^- \cdot 2H_2O$, **1**)

Several efficient methods for the syntheses of quinazoline derivatives have been developed [9—12], and hence the synthetic access to DOP was well established when we initiated our investigation. The first structural results of DOP hydrochloride **1** were already available: the crystal structure of anhydrous DOP hydrochloride was determined by A.G. Tojiboev *et al.* [13], and B. Tashkhodzhaev *et al.* [14] published the results on the corresponding dihydrate in the space group $Pna2_1$. These earlier studies revealed the essential geometric parameters of the compound, but they were obtained at room temperature and were limited with respect to resolution and accuracy. We here wish to communicate the results obtained on a hitherto unknown crystal form of **1**. Its crystal quality proved to be suitable for an experimental charge density determination of this biochemically relevant scaffold. The charge density study is based on a multipole refinement [15] of intensities from a high-resolution single crystal X-ray diffraction experiment. It is followed by a topological analysis providing the derivation of the electrostatic properties of the constituents and details of intra- and intermolecular interactions.

EXPERIMENTAL

Following the method of Shakhidoyatov [9], 2,3-Trimethylen-3,4-dihydroquinazolin-4-one (Deoxyvazicinone) was synthesized by condensation of anthranilic acid with γ-butyrolactam in the presence of phosphoroxychloride. Yield 83.8 %, m.p. 110—111 °C.

Synthesis of 2,3-trimethylen-3,4-dihydroquinazoline hydrochloride. 1.86 g (0.01 mol) of 2,3-trimethylen-3,4-dihydroquinazolin-4-one was placed in a flat-bottomed flask. 31.5 ml (20 %) of hydrochloric acid was added. Over a period of 3 h, 6.5 g (0.1 mol) of Zn powder was added in small quantities under stirring. After the addition of Zn, the stirring was continued and the reaction mixture was kept at 100 °C on a water bath for 5 h. After this time the excess of Zn was filtered and the filtrate was allowed to crystallize at 6 °C. After 12 h the precipitate was recovered by filtration and solid **1** was recrystallized from ethanol. Yield 95.5 % (2 g).

Colorless single crystals of high quality were obtained by recrystallization from ethanol at 10 °C. X-ray intensity data were collected at 100 K with MoK_α radiation from an INCOATEC microsource (λ = 0.71073 Å) on a Bruker D8 goniometer equipped with an APEX CCD detector. An Oxford Cryosystems 700 controller was used to ensure the constant temperature during data collection. Frames were collected in a ω-scan mode in nine runs with different settings for the detector angle θ and crystal rotation ϕ and integrated with the help of the SAINT program [16]. A multi-scan absorption correction was performed with SADABS [17]. The structure was solved by direct methods with SHELXS97 [18]. The refinement on F^2 at the Independent Atom Model (IAM) level was conducted with SHELXL-97 [18]. Anisotropic displacement parameters were assigned to non-hydrogen atoms. The positional coordinates of H atoms attached to C and N were refined freely, and their isotropic displacement parameters were set to $1.2U_{eq}$ of the corresponding parent atoms; for H atoms associated with the water molecules, the O—H distances were restrained to 0.84 Å, and their isotropic displacement parameters were also set to $1.2U_{eq}$ of the corresponding oxygen atoms. A satisfactory enantiomorph polarity parameter [19] was obtained.

Multipole refinements on F^2 based on the Hansen—Coppens formalism for the aspheric atomic density expansion [15] were carried out with the XD2006 program [20]. Multipoles up to hexadecapoles for Cl, O, N, and C atoms and multipoles up to quadrupoles for the H atoms involved in hydrogen bonding were refined; for the remaining H atoms, multipoles up to bond-oriented dipoles were considered. For the final model of the structure, the rigid bond test [21] was satisfactory, with a maximum difference in the mean-square displacement amplitudes along a covalent bond of 0.0020(5) Å^2. Crystal data, data collection parameters and convergence results have been compiled in Table 1. Diagrams related to the data quality and completeness are available in the Supporting Information. Crystallographic data for **1** in CIF format are available: CCDC 864060 (independent atom model) and CCDC 864061 (multipole model).

Table 1

Crystal data, data collection parameters, and convergence results for $DOPH^+ Cl^- \cdot 2H_2O$, **1**

Chemical formula	$C_{11}H_{17}N_2ClO_2$	Refinement	IAM model
M_r	244.72	Function minimized	F^2
Crystal system, space group	Orthorhombic, $P2_12_12_1$	$R(>2\sigma)$, $wR2(>2\sigma)$, $wR2_{all}$, S	0.058, 0.131, 0.156, 1.039
Temperature, K	100	No. reflections in refinement	15230
a, b, c, Å	6.9445(6), 9.6917(8), 17.9575(15)	No. of parameters	196
V, Å^3	1208.61(18)	$\Delta\rho_{max}$, $\Delta\rho_{min}$, e·Å^{-3}	0.712, –0.321
Z	4	Flack parameter (Flack, 1983)	0.04(4)
Radiation type	MoK_α		
μ, mm^{-1}	0.304	Refinement	Multipole model
Crystal form, size, mm	Plate, 0.30×0.30×0.08	Function minimized	F^2
		$R(>2\sigma)$, $wR2(>2\sigma)$, $wR2_{all}$, S	0.046, 0.091, 0.121, 1.069
Data collection			
Diffractometer	Bruker APEX CCD	No. reflections in refinement	15229
Data-collection method	ω scans	No. of parameters	656
Absorption correction	Multi-scan	$(\sin\theta/\lambda)_{max}$, Å^{-1}	1.151
T_{max}, T_{min}	0.9761, 0.9143	$\Delta\rho_{max}$, $\Delta\rho_{min}$, e·Å^{-3}	0.413, –0.348
No. of measured, independent and observed reflections	74991, 15230, 8657		
		Contraction parameters	Multipole model
Criterion for observed reflections	$I > 2\sigma(I)$	κ	Cl: fixed to 1.0; C, N, O, H: refined
R_{int}	0.0774	κ′ (non-H atoms)	Refined
θ_{max}, deg.	54.9	κ′ (H atoms excl. H1)	Fixed to 1.0

Theoretical calculations were based on density functional theory. The Gaussian09 program system [22] was used to perform a single-point calculation based on the experimental X-ray structure of **1** with a b3lyp/aug-cc-pvdz basis [23].

RESULTS AND DISCUSSION

$DOPH^+ Cl^- \cdot 2H_2O$ crystallizes in the orthorhombic space group $P2_12_12_1$ with a protonated quinazolinium cation, a chloride anion, and two hydrate water molecules in the asymmetric unit.

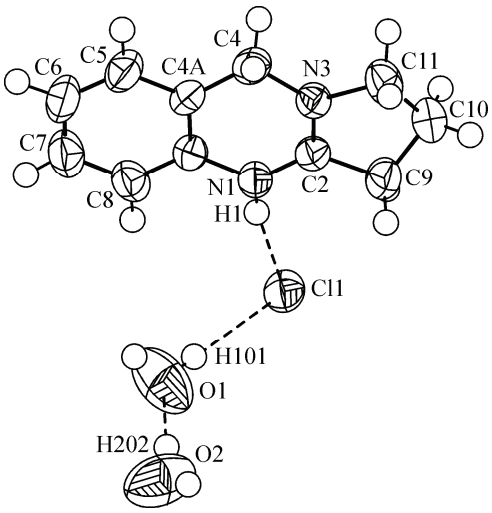

Fig. 2 shows a displacement ellipsoid plot of the asymmetric unit.

The cationic moiety is almost planar; the only exception is the C10 methylene group in the five-membered alicycle, which is displaced by 0.326(2) Å out of the least-squares plane through the other non-hydrogen atoms of the cation. The protonated N1 nitrogen atom in the cation interacts with its closest anionic chloride neighbor *via* a relatively short N—H···Cl bond characterized by a donor···acceptor distance of 3.0968(8) Å.

Fig. 2. Displacement ellipsoid plot [24] of a pair of cations and anions in **1**.
Ellipsoids are drawn at 90 % probability; H atoms are shown as spheres with an arbitrary radius

When viewed along the shortest lattice constant *a*, the crystal packing is characterized by stacking of the heterocyclic cations. Polar and apolar moieties segregate in the crystal, with the chloride anions and water molecules filling the channels formed between the organic residues (Fig. 3).

Not only the N—H moiety in the cation, but all other potential donor functionalities are engaged in classical hydrogen bonds, as well: one-dimensional ribbons of hydrogen-bonded water molecules and chloride anions extend along the crystallographic [100] direction. Fig. 4 shows such a ribbon in the *ac* plane.

The high resolution of our experimental X-ray data allows for a more detailed discussion of chemical bonding. After the convergence of the standard spherical model, a difference Fourier synthesis showed that due to covalent bonds the electron density is accumulated between all atoms in the tricyclic cation. The diffraction data were of sufficient quality for an atom-centered multipole refinement. We have interpreted the resulting experimental electron density in terms of Bader′s Atoms in Molecules approach [25]. All intramolecular bonds in the cationic residue and water molecules are associated with (3, –1) critical points. The electron density and its Laplacian in these so-called bond critical points (BCPs) reflect the covalent character and the bond order. A Laplacian of the electron density in the plane of the heterocyclic cation (defined by C2, C4A, and C8A) is given in Fig. 5 and shows negative values, corresponding to essentially covalent bonding, for all conventional chemical bonds in these residues.

We have recently been able to confirm that very short O—H···O interactions can be associated with an at least partially covalent character [26], whereas the hydrogen bonds in general have a more electrostatic character [27] and therefore can be regarded as essentially closed shell interactions. This also applies for $DOPH^+$ $Cl^-\cdot 2H_2O$: the shortest and presumably strongest N1—H1···Cl1 hydrogen bond is characterized by an electron density of 0.21(2) $e\cdot Å^{-3}$ and a positive value of 1.83(2) $e\cdot Å^{-5}$ for the Laplacian in BCP of its H···acceptor part.

Close to the center of each ring in the tricyclic cation, a (3, +1) or ring critical point is located. Both ring and bond critical points may readily be identified in a gradient trajectory plot of the electron density (Fig. 6).

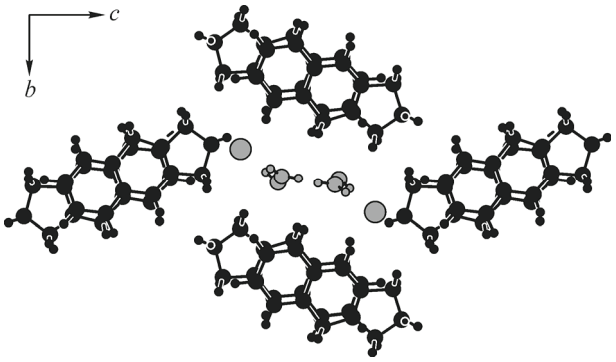

Fig. 3. Packing in $DOPH^+$ $Cl^-\cdot 2H_2O$; the tricyclic cations are shown in black, the polar chloride and aqua residues in grey

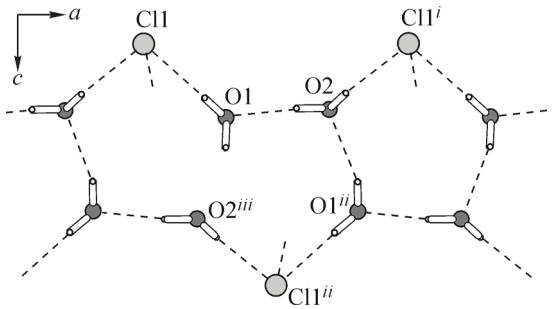

Fig. 4. Hydrogen bonding between the chloride anions and water molecules in **1**; cations have been omitted. Donor···acceptor distances [E]: Cl1···O1 3.1727(15); O1···O2 2.712(2); O1···O2^{iii} 2.800(2); Cl1^{i}···O2 3.1377(16).
Symmetry operators: $i = 1 + x, y, z$; $ii = x + 1/2, 1/2 - y, 2 - z$; $iii = x - 1/2, 1/2 - y, 2 - z$

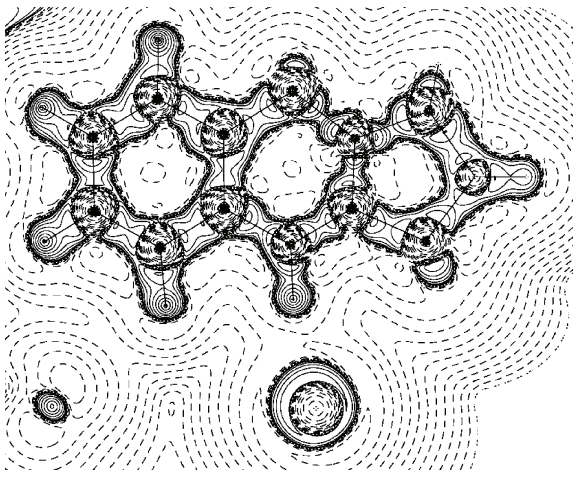

Fig. 5. Laplacian of the electron density ($\pm 2^n \times 10^{-3}$ $eÅ^{-5}$ ($0 \le n \le 20$), positive contours dashed, negative contours solid lines)

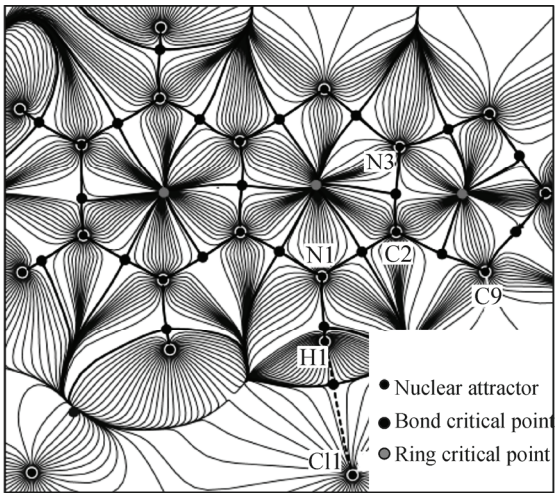

Fig. 6. Representation of the gradient field of the total electron density in the cation plane with nuclear attractors; BCPs and ring critical points

Our main focus was on the charge distribution and the electrostatic potential of the compound. A representation of the electrostatic potential [28] is shown in the graphical abstract of this article.

Based on the experimental charge density, the formally anionic chloride results indeed as the most negatively charged atom. The positive charge in the cation is distributed over the protonated N1 site and the hydrogen atoms in the heteroaromatic cation. A full list of multipole populations of the refinement has been compiled in the Supporting Information. According to our experimental charge density, the dipole moment of an ion pair in the extended structure, i.e. a hydrogen-bonded aggregate of the neighbouring $DOPH^+$ and Cl^- ions, amounts to 16.1 D. The direction of this experimental moment is not immediately intuitive, but rather influenced by the arrangement of the ions and their polarization by the surrounding residues in the crystal. For comparison with a hypothetical gas phase situation, we used the geometry from the experimental X-ray structure to generate a DOP—H···Cl adduct and obtained its electron density from a single point calculation. For such an isolated adduct, a significantly smaller dipole moment of 10.2 D, almost coinciding with the chlorine-nitrogen vector, is obtained. We conclude that both modulus and direction of the dipole moment strongly depends on the arrangement of the formally ionic constituents and the polar solvent in the crystal. In view of the recent results by Engels and coworkers [29], such a discrepancy is not surprising. The experimental result from the molecular crystal may well be a better approximation to the real situation in an unknown and biologically relevant complex between the pharmaceutically active compound and its receptor than a gas-phase calculation.

Acknowledgments. This work was supported by the German Academic Exchange Service (DAAD), Germany and by DFG, priority program 1178, Experimental Charge Density as the Key to Understand Chemical Interactions.

REFERENCES

1. *Johne S.* // Pharmazie. – 1981. – **36**. – P. 583.
2. *Telezhenetskaya M.V., Yunusov S.Yu.* // Chem. Natur. Comp. – 1977. – **13**, N 6. – P. 731.
3. *Yunusov S.Yu., Tulyaganov N., Telezhenetskaya M.V. et al.* // USSR Patent No. 605614, Anticholinesterase agent, Byull. Izobret. (Russ.). – 1978. – P. 17.
4. *Harris C.S., Hennequin L., Morgentin R. et al.* // Targets in Heterocyclic Systems. – 2010. – **14**. – P. 315.
5. X-ray Charge Densities and Chemical Bonding / P. Coppens. – New York: Oxford University Press, 1997.
6. *Mebs S., Lueth A., Loewe W. et al.* // Zeitschrift für Kristallographie. – 2008. – **223**, N 8. – S. 502.
7. *Khaliq T., Misra P., Gupta S. et al.* // Bioorg. Med. Chem. Lett. – 2009. – **19**, N 9. – P. 2585.
8. *Khashimov Kh.N., Telezhenetskaya M.V., Yunusov S.Yu.* // Chem. Natur. Comp. – 1969. – **5**, N 5. – P. 456.
9. *Shakhidoyatov Kh.M., Irisbaev A., Yun L.M. et al.* // Chem. Heterocycl. Comp. – 1976. – **12**, N 11. – P. 1286.
10. *Shakhidoyatov Kh.M., Kaisarov I.K.* // Chem. Natur. Comp. – 1998. – **34**, N 1. – P. 59.
11. *Jahng K.C., Kim S.I., Kim D.H. et al.* // Chem. Pharm. Bull. – 2008. – **56**, N 4. – P. 607.
12. *Al-Shamma A., Drake S., Flynn D.L. et al.* // J. Nat. Prod. – 1981. – **44**, N 6. – P. 745.
13. *Tojiboev A.G., Turgunov K.K., Tashkhodjaev B. et al.* // Chem. Natur. Comp. – 2006. – **42**, N 3. – P. 280.
14. *Tashkhodzhaev B., Molchanov L.V., Turgunov K.K. et al.* // Chem. Natur. Comp. – 1995. – **31**, N 3. – P. 421.
15. *Hansen N.K., Coppens P.* // Acta Crystallogr. Sect. A. – 1978. – **34**. – P. 909.
16. SMART and SAINT. – USA, Bruker AXS Inc., Madison, Wisconsin, 1999.
17. SADABS: Program for Empirical Absorption Correction of Area Detector Data, V 2004/1. – USA, Bruker AXS Inc.: Madison, WI, 2004.

18. *Sheldrick G.M.* // Acta Crystallogr. Sect. A. – 2008. – **64**. – P. 112.
19. *Flack H.D.* // Acta Crystallogr. Sect. A. – 1983. – **39**, N 6. – P. 876.
20. *Volkov A. et al.* XD2006. – USA, University of New York at Buffalo, 2006.
21. *Hirshfeld F.L.* // Acta Crystallogr. Sect. A. – 1976. – **32**, N 2. – P. 239.
22. *Frisch M.J. et al.* Gaussian 09, Revision A-02. – the USA, Gaussian, Inc.: Wallingfort CT, 2009.
23. *Dunning T.H.* // J. Chem. Phys. – 1989. – **90**, N 2. – P. 1007.
24. *Spek A.L.* // Acta Crystallogr. Sect. D. – 2009. – **65**, N 2. – P. 148.
25. Atoms in Molecules — a Quantum Theory / R.F.W. Bader. – Oxford: Clarendon Press, 1990.
26. *Serb M., Wang R., Meven M. et al.* // Acta Crystallogr. Sect. B. – 2011. – **67**, N 6. – P. 552.
27. *Gilli P., Bertolasi V., Ferretti V. et al.* // J. Amer. Chem. Soc. – 1994. – **116**, N 3. – P. 909.
28. *Hübschle C.B., Dittrich B.* // J. Appl. Crystallogr. – 2011. – **44**, N 1. – P. 238.
29. *Mladenovic M., Arnone M., Fink R.F.* // J. Phys. Chem. – 2009. – **113**, N 15. – P. 5072.